

---

# PENTACLE: Parallelized Particle-Particle Particle-Tree Code for Planet Formation

Masaki IWASAWA,<sup>1,\*</sup> Shoichi OSHINO,<sup>2</sup> Michiko S. FUJII,<sup>3</sup> and Yasunori HORI<sup>4,5</sup>

<sup>1</sup>Advanced Institutes for Computational Science, Minatojima-minamimachi, Chuo-ku, Kobe, Hyogo 6500047, Japan

<sup>2</sup>Centre for Computational Astrophysics, National Astronomical Observatory of Japan, 2-21-1 Osawa, Mitaka, Tokyo 1818588, Japan

<sup>3</sup>Department of Astronomy, Graduate School of Science, The University of Tokyo, 7-3-1 Hongo, Bunkyo-ku, Tokyo 1130033, Japan

<sup>4</sup>Astrobiology Centre, National Institutes of Natural Sciences, 2-21-1 Osawa, Mitaka, Tokyo 1818588, Japan

<sup>5</sup>Exoplanet Detection Project, National Astronomical Observatory of Japan, 2-21-1 Osawa, Mitaka, Tokyo 1818588, Japan

\*E-mail: masaki.iwasawa@riken.jp

Received (reception date); Accepted (acceptation date)

## Abstract

We have newly developed a Parallelized Particle-Particle Particle-tree code for Planet formation, PENTACLE, which is a parallelized hybrid  $N$ -body integrator executed on a CPU-based (super)computer. PENTACLE uses a 4th-order Hermite algorithm to calculate gravitational interactions between particles within a cutoff radius and a Barnes-Hut tree method for gravity from particles beyond. It also implements an open-source library designed for full automatic parallelization of particle simulations, FDPS (Framework for Developing Particle Simulator) to parallelize a Barnes-Hut tree algorithm for a memory-distributed supercomputer. These allow us to handle 1 – 10 million particles in a high-resolution  $N$ -body simulation on CPU clusters for collisional dynamics, including physical collisions in a planetesimal disc. In this paper, we show the performance and the accuracy of PENTACLE in terms of  $\tilde{R}_{\text{cut}}$  and a time-step  $\Delta t$ . It turns out that the accuracy of a hybrid  $N$ -body simulation is controlled through  $\Delta t/\tilde{R}_{\text{cut}}$  and  $\Delta t/\tilde{R}_{\text{cut}} \sim 0.1$  is necessary to simulate accurately accretion process of a planet for  $\geq 10^6$  years. For all those who interested in large-scale particle simulations, PENTACLE customized for planet formation will be freely available from <https://github.com/PENTACLE-Team/PENTACLE> under the MIT licence.

**Key words:** Methods: numerical<sub>1</sub> – Planets and satellites: formation<sub>2</sub>

---

## 1 Introduction

Planet formation proceeds via collisions and accumulation of planetesimals. Planetesimals, which are larger than neighbours, can be predators because of stronger gravitational focusing. During this early phase, larger planetesimals overwhelm smaller planetesimals, growing rapidly in an exponential fash-

ion (Wetherill & Stewart 1989). However, the growth of a large planetesimal, the so-called planetary embryo, slows down because of the increase in random motions of small planetesimals around itself by gravitational scattering (Ida & Makino 1993). At this stage, planetary embryos grow oligarchically to be similar-size and then, their orbital separations become  $\sim 10$

times Hill radii as a result of orbital repulsion. A series of pathways toward planet formation are commonly known as runaway growth and oligarchic growth (Kokubo & Ida 1998).

Collisional dynamics in a swarm of planetesimals is controlled by their mutual gravity. Planetesimal accretion is a non-linear dynamical process via multi-body interactions. An  $N$ -body simulation is an effective means of examining dynamical behaviours of particles that gravitationally interact each other. Gravitational force has an infinite range, whereas gravitational interactions between particles undergoing close encounters regulate the length of a time-step to integrate the dynamical evolution of a collisional system. As a result, a direct  $N$ -body simulation for planet formation requires  $O(N^2)$  integrations per short time-step.

Due to a high computational cost of direct  $N$ -body simulations, we can handle at most  $\sim 10^4 - 10^5$  particles in simulations of terrestrial planet formation, as shown in Fig. 1. The size of an equal-mass planetesimal initially assumed in such  $N$ -body simulations is typically several hundred kilometres in radius, which is similar to that of 1 Ceres and 4 Vesta. The observed population of asteroids in the main asteroid belt suggests that the smaller asteroids are, the more abundant they are (e.g. see Fig. 1 in Bottke et al. 2005). Although the present-day size distribution of asteroids reflects the combination of a long-term evolution of collisional processes and gravitational perturbations from the planets, there were likely numerous small bodies at the early stage of planet formation. In order to describe the dynamical behaviours of small bodies in an  $N$ -body simulation, we need to improve the mass resolution of particles. A classical way is to introduce a statistical method that describes accumulation processes of planetesimals in a sea of small bodies, following a collisional probability; for instance, statistical simulations (e.g. Weidenschilling et al. 1997; Inaba et al. 2001; Kobayashi et al. 2011), hybrid  $N$ -body simulations with a statistical method for small bodies (e.g. Bromley & Kenyon 2006; Chambers 2008), and super-particle approximations (Levison et al. 2012; Morishima 2015).

Another tractable approach is to increase the number of particles ( $N$ ) in an  $N$ -body simulation. There were several attempts to accelerate and optimize processes of computing gravitational interactions between particles. Specialized hardwares such as HARP and GRAPE (e.g. Sugimoto et al. 1990; Makino et al. 1993; Makino et al. 2003) were developed to accelerate the calculation of gravitational forces, dramatically increasing the number of particles used in direct  $N$ -body simulations. Recently, Graphic Processing Units (GPUs) have been introduced as an alternative accelerator (e.g. Wang et al. 2015; Bédorf et al. 2015). However, the upper limit of  $N$  was still several tens of thousands due to the small time-steps for close encounters and relatively long integration time (more than one million orbital times at 1 au), which results in a large num-

ber of steps.

In contrast, tree methods (Barnes & Hut 1986) can reduce the computational cost of gravity parts to  $O(N \log N)$ . PKDGRAV (Stadel 2001) optimized for parallel computers adopts a tree method with variable time-steps. Using PKDGRAV, Richardson et al. (2000) simulated the dynamical evolution of a million planetesimals for only hundreds of dynamical times. Tree codes and also a family of particle-mesh scheme such as the  $P^3M$  scheme (Hockney & Eastwood 1981), and combinations of the  $P^3M$  and tree methods (Xu 1995; Bagla 2002; Dubinski et al. 2004; Springel 2005; Yoshikawa & Fukushige 2005; Ishiyama et al. 2009) can treat extremely large numbers of particles, and therefore they are used for cosmological simulations. While dark matters can be considered as a collisionless system, planetesimal-planetesimal interactions are collisional. If cosmological  $N$ -body codes are applied to planetary accretion, small time-steps for close encounters and a large number of steps become a bottleneck.

A mixed-variable symplectic (MVS) integrator, in which a Hamiltonian is split into two parts and integrated separately, is another direction to manipulate the calculation cost (Wisdom & Holman 1991; Kinoshita et al. 1991). In a MVS integrator, gravitational interactions caused by close encounters are integrated using a higher-ordered scheme with smaller time steps, but the others are calculated using a Kepler solver or a fast scheme such as a tree method. SyMBA (Duncan et al. 1998), Mercury (Chambers 1999), and  $P^3T$  method (Oshino et al. 2011) incorporate this method, albeit the way to split a Hamiltonian is different among them. Also, the combination of these attempts would be possible. GENGA (Grimm & Stadel 2014) used GPUs for computing gravity parts, adopting a MVS method as an integrator. Oshino et al. (2011) applied  $P^3T$  method to GRAPE and later, Iwasawa et al. (2015) developed a GPU-enabled  $P^3T$  method and succeeded in handling more than a million particles, although they considered a star cluster model in their simulation.

We newly develop a parallelized  $N$ -body integrator based on  $P^3T$  method (Oshino et al. 2011), a Parallelized Particle-Particle-Particle-tree code for Planet formation which is called PENTACLE hereafter. This hybrid  $N$ -body code allows us to perform a high-resolution  $N$ -body simulation with 1 – 10 million particles in a collisional system such as a planetesimal disc for  $\sim 1$  Myr on a standard supercomputer.

In this paper, we present our new hybrid  $N$ -body code, PENTACLE, in Section 2. We show the performance and accuracy of PENTACLE in terms of a cut-off radius and a time-step in Section 3 and also demonstrate  $N$ -body simulations of planetary accretion in a swarm of 1 million planetesimals. We summarize our paper in the last section.

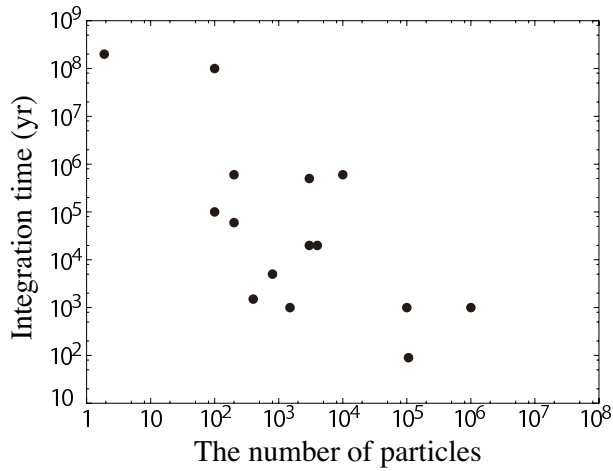


**Fig. 1.** History of  $N$ -body simulations for terrestrial planet formation (see Richardson et al. (2000) and references therein). The current level of the number of particles used in  $N$ -body simulations of planet formation is  $\sim 10^4 - 10^5$ .

## 2 Methods

In this section, we present a basic concept and algorithm of PENTACLE. In section 2.1, we briefly review the Particle-Particle Particle-Tree ( $P^3T$ ) method which is a hybrid symplectic integrator used in PENTACLE. In sections 2.2.1 and 2.2.2, we describe a parallelization method for computing gravity forces between particles. In the last section, we show the actual recipe of PENTACLE.

### 2.1 Particle-Particle Particle-Tree method

The concept of PENTACLE comes from the  $P^3T$  method (Oshino et al. 2011). The  $P^3T$  method is a hybrid symplectic integrator such as SyMBA (Duncan et al. 1998) and Mercury (Chambers 1999). The basic idea of this hybrid symplectic integrator is to split a gravitational force between two particles, i.e., a Hamiltonian, into two parts (soft and hard parts) by their distance in heliocentric coordinates. The Hamiltonian used in  $P^3T$  is given by

$$\begin{aligned}
 H &= H_{\text{hard}} + H_{\text{soft}}, \\
 H_{\text{hard}} &= \sum_i^N \left[ \frac{|\mathbf{p}_i|^2}{2m_i} - \frac{Gm_i m_0}{r_{i0}} \right] - \sum_i^N \sum_{i < j}^N \frac{Gm_i m_j}{r_{ij}} [1 - W(r_{ij})], \\
 H_{\text{soft}} &= - \sum_i^N \sum_{i < j}^N \frac{Gm_i m_j}{r_{ij}} W(r_{ij}), \\
 \mathbf{q}_{ij} &= \mathbf{q}_i - \mathbf{q}_j, \\
 r_{ij} &= |\mathbf{q}_{ij}|,
 \end{aligned}$$

where  $G$  is the gravitational constant,  $m_i$ ,  $\mathbf{p}_i$ , and  $\mathbf{q}_i$  are the mass, momentum and position of an  $i$ -th particle, and the subscript 0 indicates the Sun. To connect between a short-range

and a long-range forces smoothly, we introduce a cutoff function  $W(r_{ij})$  defined as

$$W(y; \gamma) = \begin{cases} \frac{7(\gamma^6 - 9\gamma^5 + 45\gamma^4 - 60\gamma^3 \log \gamma - 45\gamma^2 + 9\gamma - 1)}{3(\gamma - 1)^7} y & (y < \gamma) \\ f(y; \gamma) + (1 - f(1; \gamma))y & (\gamma \leq y < 1) \\ 1 & (1 \leq y) \end{cases} \quad (6)$$

$$\begin{aligned}
 f(y; \gamma) &= (-10/3y^7 + 14(\gamma + 1)y^6 - 21(\gamma^2 + 3\gamma + 1)y^5 \\
 &\quad + (35(\gamma^3 + 9\gamma^2 + 9\gamma + 1)/3)y^4 \\
 &\quad - 70(\gamma^3 + 3\gamma^2 + \gamma)y^3 \\
 &\quad + 210(\gamma^3 + \gamma^2)y^2 - 140\gamma^3 y \log(y) \\
 &\quad + (\gamma^7 - 7\gamma^6 + 21\gamma^5 - 35\gamma^4)) / (\gamma - 1)^7, \quad (7)
 \end{aligned}$$

$$\gamma = \frac{r_{\text{in}}}{r_{\text{out}}}, \quad (8)$$

$$y = \frac{r_{ij}}{r_{\text{out}}}, \quad (9)$$

where  $r_{\text{out}}$  and  $r_{\text{in}}$  are the outer and inner cutoff radii (see Iwasawa et al. 2015). This cutoff function approaches asymptotically zero if  $r_{ij} < r_{\text{in}}$  and becomes unity if  $r_{ij} > r_{\text{out}}$ . In PENTACLE, we use  $\gamma = 0.1$ . Forces derived from the two components of the Hamiltonian are given by

$$\mathbf{F}_{\text{hard}, i} = - \frac{\partial H_{\text{hard}}}{\partial \mathbf{q}_i} \quad (10)$$

$$= - \sum_{j \neq i}^N \frac{Gm_i m_j}{r_{ij}^3} [1 - K(r_{ij})] \mathbf{q}_{ij} - \frac{Gm_i m_0}{r_{i0}^3} \mathbf{q}_{i0}, \quad (11)$$

$$\mathbf{F}_{\text{soft}, i} = - \frac{\partial H_{\text{soft}}}{\partial \mathbf{q}_i} = - \sum_{j \neq i}^N \frac{Gm_i m_j}{r_{ij}^3} K(r_{ij}) \mathbf{q}_{ij}, \quad (12)$$

$$K(x) = \begin{cases} 0 & (x < 0) \\ -20x^7 + 70x^6 - 84x^5 + 35x^4 & (0 \leq x < 1) \\ 1 & (1 \leq x) \end{cases} \quad (13)$$

$$x = \frac{y - \gamma}{1 - \gamma}. \quad (14)$$

A formal solution of the canonical equation of motion for a given Hamiltonian  $H$  is given by

$$\mathbf{w}_i(t + \delta t) = e^{\delta t \{, H\}} \mathbf{w}_i(t) = e^{\delta t \{, H_{\text{soft}} + H_{\text{hard}}\}} \mathbf{w}_i(t), \quad (15)$$

$$\mathbf{w}_i = (\mathbf{q}_i, \mathbf{p}_i), \quad (16)$$

- (1) where  $\mathbf{w}_i$  is the canonical variable of an  $i$ -th particle in phase space and  $\{, \}$  means the Poisson bracket. In PENTACLE, we integrate time evolution of  $\mathbf{w}_i$  with a second-order approximation.
- (2) If a particle of which the nearest neighbour is farther than  $r_{\text{out}}$ ,
- (3) it interacts only with the Sun and its motion is calculated by solving the Kepler equation.
- (4)
- (5) For the hard part, the  $P^3T$  method adopts a fourth-order Hermite scheme (Makino 1991) with an individual time-step method (Aarseth 1963). The individual time-step method allows us to handle readily close encounters and physical collisions. When  $r_{\text{out}}$  is equal to the Hill radius of a particle, most

particles have no counterpart inside  $r_{\text{out}}$ . The number of integration for the hard part is  $O(N)$  per time-step, whereas that for the soft part is  $O(N^2)$ . Thus, we apply the Barnes-Hut tree method (Barnes & Hut 1986) (with up to the quadrupole moment) to the P<sup>3</sup>T, which reduces a computational cost from  $O(N^2)$  to  $O(N \log N)$ . We also create a list of neighbours based on a tree structure in order to evaluate efficiently forces from the hard part.

## 2.2 Parallelization of PENTACLE

### 2.2.1 The soft part of a gravity force

One of essential ingredients to perform large  $N$ -body simulations is parallelization for calculating gravitational interactions between particles. We apply a parallelization method executed on distributed-memory parallel computers to PENTACLE. This method consists of the following steps.

1. A computational domain is divided into sub-domains, each of which is allocated to one MPI process.
2. Particles are assigned to each process, and a tree structure is constructed in it.
3. Based on the tree structures, processes provide information of particles, i.e., multipole moments of a gravitational potential, to each other [here after this step is called “exchange Local Essential Tree(LET)”].
4. Using the information received at previous step, reconstruct entire tree structures on each process.
5. Each process evaluates gravity forces between particles using the tree structure and integrates the motions of their assigned particles by using a leapfrog scheme and a fixed time-step.

In order to efficiently implement this scheme, we use a library called FDPS (see Iwasawa et al. 2016). FDPS is a C++ template library that helps users develop parallel particle-based simulation codes. The basic idea of FDPS is to separate technical parts involved in parallelization from the physical problem itself: specifically, the decomposition of a computational domain into sub-ones, exchanging particles among inter-processes, and gathering information of particles stored in other processes. FDPS provides functions necessary for parallelized tree-codes as C++ templates. Thus, users just define an arbitrary data structure and kernel function of a potential between two interacting particles, and then FDPS takes care of data exchanges among processes. In PENTACLE, we utilize a cutoff function,  $\mathbf{K}(\mathbf{r}_{ij})$ , as a kernel function of gravitational interactions between particles.

FDPS also has APIs to search for neighbouring particles; for example, we can use `getneighbourListOneParticle()` to find particles within the radius of  $r_{\text{out}}$  around a given particle.

### 2.2.2 The hard part of a gravity force

Parallelization of the hard part in PENTACLE is more straightforward. If particles has no neighbour within  $r_{\text{out}}$ , their motions can be individually integrated by solving the Kepler equation on each process. We use the Newton-Raphson method to solve the Kepler equation in this scheme. For convenience, we introduce the term “cluster” which is defined as a subset of particles. Each particle must belongs to a cluster and clusters are exclusive each other. All neighbour particles of an arbitrary particle in a given cluster belong to the same cluster. In other words, a particle out of a given cluster dose not have neighbours in this cluster. We also define the size of cluster as the number of particles in a given cluster and refer a cluster with the size of  $k$  as  $k$ -cluster. Thus a particle with no neighbours is in a 1-cluster.

When a particle has a neighbour and its neighbour is the target particle only (i.e. the both particles are in a 2-cluster), the particle interacts only with its neighbour and the Sun. This system can be considered as an isolated three-body system. If both particles are loaded on the same process, any inter-process communication is not required. Otherwise, we just send the particle’s data to the process in which its neighbour is stored.

In principle, we can integrate the motion of a particle with multiple neighbours in a similar way. It, however, is a little bit complicated to find a cluster with the size  $\geq 2$  (hereafter  $k_{>2}$ -cluster) in parallel. We first send particles in  $k_{>2}$ -cluster to the root process named as “rank 0” and the root process integrates their motions in serial order. As shown later, particles in  $k_{>2}$ -cluster are rare and this serial procedure has little effect on the scaling performance of PENTACLE for  $N \lesssim 10^6$ .

## 2.3 Procedures in PENTACLE

The actual calculation of an  $N$ -body simulation in PENTACLE proceeds as follows;

1. Define a data structure of a particle and a kernel function of gravitational interactions between particles.
2. Send particles’ data to FDPS.
3. FDPS returns the soft force and the number of neighbours for each particle.
4. Each process gives all the assigned particles their kick velocities using their soft forces.
5. According to the number of neighbours, particles are classified into three groups: a non-neighbour, one-neighbour, and multiple-neighbour group.
6. Each process integrates the motion of particles without neighbours, the so-called drift-step, by solving the Kepler equation.
7. If a particle has a neighbour, each process checks if the neighbour’s neighbour is the target particle only, i.e., a referred particle. If the referred and neighbour particles are assigned to the same process, the two are integrated in their

process, using a fourth-order Hermite scheme. If not, the referred particle is sent to the neighbour's process and both processes integrate their motions. If the neighbour has  $\geq 2$  neighbours, the referred particle is sent to the process with rank 0 (the root process).

8. Each process sends particles with  $\geq 2$  neighbours to the root process.
9. The root process integrates all the particles received.
10. The root process returns particles' data to their original processes.

### 3 Results

We demonstrate planetary accretion in a swarm of planetesimals by using PENTACLE. Our simulations start from a system of equal-mass planetesimals with mean density of  $2 \text{ g cm}^{-3}$  in a gas-free environment. We use the minimum mass solar nebula model (Hayashi 1981) as a nominal surface density profile of solid material,  $\Sigma_{\text{solid}}$ , given by

$$\Sigma_{\text{solid}} = 10 \eta_{\text{ice}} \left( \frac{a}{1 \text{ au}} \right)^{3/2} \text{ g cm}^{-2}, \quad (17)$$

where  $a$  is the semi-major axis and  $\eta_{\text{ice}}$  is the enrichment factor of a surface density of solid material beyond a snow line ( $a_{\text{snow}} = 2.7 \text{ au}$ ) due to ice condensation.

We consider two planetesimal disc models for benchmark tests. One is a narrow ring model (model R) between 0.95 au and 1.05 au and the other is a disc model (model D) with radius of 1 au – 11 au. The ring width is large enough to trace motions of planetesimals spreading out in a disc until the end of our simulations. In order to investigate impacts of a computational domain size on the applicability of our new algorithm, we use  $\eta_{\text{ice}} = 1$ . This leads to a total solid amount of  $0.236 M_{\oplus}$  for model R and that of  $10.9 M_{\oplus}$  for model D (see also Table 1).

An initial eccentricity and inclination of each planetesimal are given by a Rayleigh distribution with dispersion of  $\langle e^2 \rangle^{1/2} = 2 \langle i^2 \rangle^{1/2} = 2\sqrt{2}h$ , where  $e$  and  $i$  are the eccentricity and inclination of a planetesimal and  $h$  is the reduced Hill radius defined by the ratio of the Hill radius of a body to its semi-major axis, i.e.,  $h = r_{\text{H}}/a$ <sup>1</sup>

#### 3.1 Comparison with direct $N$ -body simulations

Assuming three different random seeds for initial values of orbital elements of planetesimals, we performed  $N$ -body simulations of  $5 \times 10^3$  planetesimals for model R. We adopted two different schemes, PENTACLE and a forth-order Hermite scheme (Makino 1991). We use  $\tilde{R}_{\text{cut}} = 0.3$ ,  $\theta = 0.5$ , and  $\Delta t = 1/64$ ,

<sup>1</sup> In the dispersion-dominated regime, a swarm of planetesimals in a Kepler potential spontaneously reach the isotropic state of  $e = 2i$  through the viscous stirring between themselves, irrespective of the initial conditions (e.g. Ida & Makino 1992).

**Table 1.** Planetesimal disc models

Name	Radius (au)	Width (au)	Total Mass ( $M_{\oplus}$ )
Model R	0.95 – 1.05	0.1	0.236
Model D	1 – 11	10	10.9

where  $\tilde{R}_{\text{cut}} = r_{\text{out}}/r_{\text{H}}$ ,  $\theta$  is the opening angle used in the P<sup>3</sup>T method (Oshino et al. 2011),  $\Delta t$  is the time-step whose unit is  $t_{\text{kep}}/2\pi$  ( $t_{\text{kep}}$  is the Kepler time), and  $r_{\text{H}}$  is the Hill radius.

Figure 2 shows that PENTACLE reproduces well results of direct  $N$ -body simulations. In all the runs, the number of remaining planetesimals decreases monotonously in a similar manner. On the other hand, we see car chases in the bottom panel of Fig. 2. Physical collisions between planetesimals are stochastic processes. As a result, mass evolution of the largest body (the so-called planetary embryo) shows a stepwise growth. In any case, we find that a planetary embryo reaches almost the same mass after  $10^4$  years. We also plot distribution functions of the eccentricity and inclination of planetesimals at  $9 \times 10^3$  year in Fig. 3. There is no significant difference for all the runs.

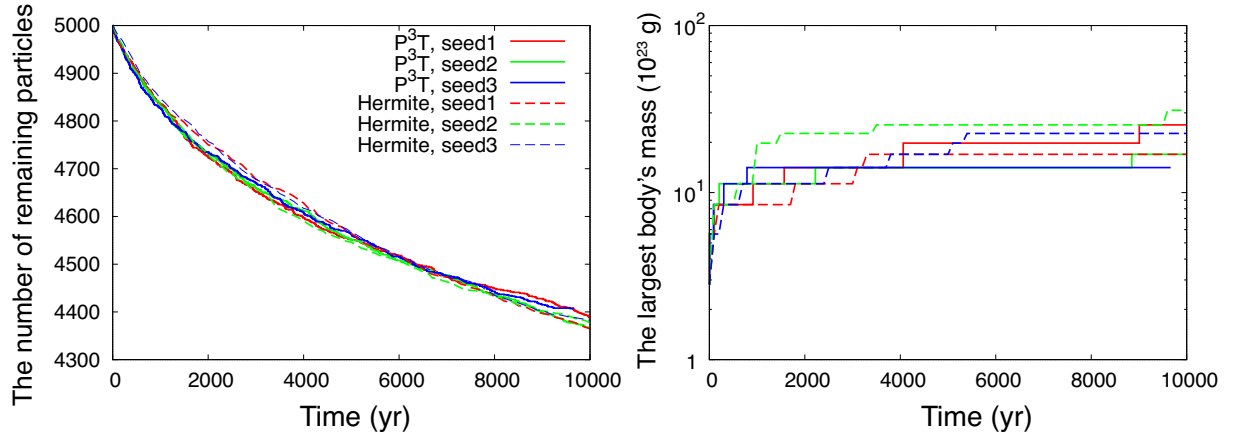
#### 3.2 Accuracy and performance

##### 3.2.1 Energy conservation

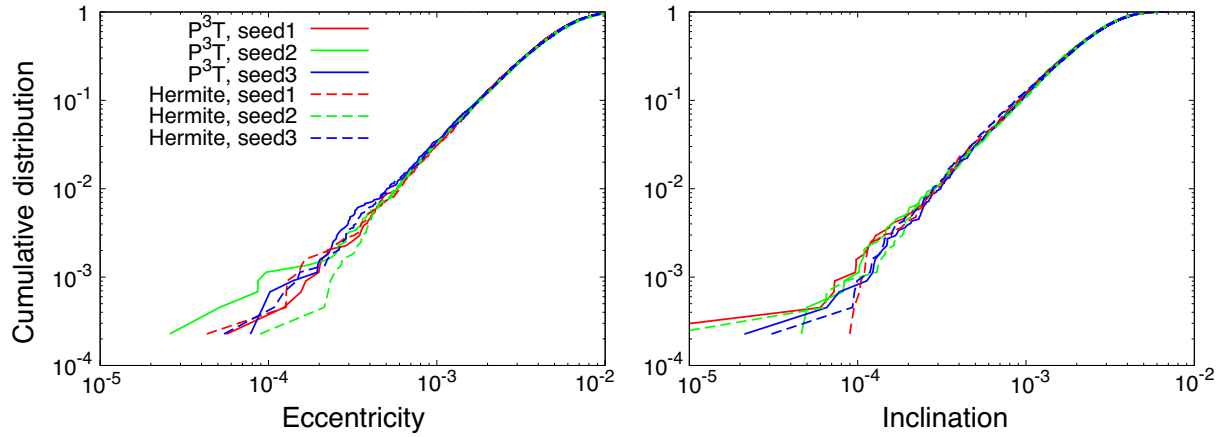
We verify energy conservation in a system of planetesimals for model R with  $N = 10^6$ . We consider two additional models with different initial velocity dispersions:  $\langle e^2 \rangle^{1/2} = 2 \langle i^2 \rangle^{1/2} = 8\sqrt{2}h$  (hot disc) and  $1/\sqrt{2}h$  (cold disc). We choose  $\theta = 0.1$  and  $\eta = 0.025$  in order to suppress energy errors which arise from both a tree approximation and a forth-order Hermite scheme, where  $\eta$  is the accuracy parameter of timesteps for the forth-order Hermite scheme (e.g. see Makino & Aarseth 1992).

Figure 4 shows the maximum relative energy error over 10 Keplerian orbits as functions of  $\Delta t$  and  $\tilde{R}_{\text{cut}}$ . For the hot disc, energy errors can be controlled through  $\Delta t/\tilde{R}_{\text{cut}}$ . This dependency is the same as that seen in a system of objects with high velocity dispersions such as star cluster simulations (Iwasawa et al. 2015). On the other hand, energy errors rather depend on  $\Delta t/(\tilde{R}_{\text{cut}})^{1.5}$  than  $\Delta t/(\tilde{R}_{\text{cut}})$  if the collisional system is cold. Energy errors of a cold system mainly come from close encounters. Since a characteristic time-scale of a close encounter is a Keplerian time, energy errors of a cold system depends on  $\tilde{R}_{\text{cut}}^{-1.5}$ . However, planetesimal discs are heated up quickly through viscous stirring and/or dynamical friction. As a result, we, *a posteriori*, can use  $\Delta t/\tilde{R}_{\text{cut}}$  as an accuracy parameter for the soft part in this paper.

Figure 5 shows time evolution of relative energy errors to 1,000 Kepler time for model R with  $N = 10^6$ ,  $\theta = 0.5$ , and  $\eta = 0.1$  with respect to five different  $\tilde{R}_{\text{cut}}$ . For all the runs, the energy errors grow gradually as  $t^{1/2}$ , as expected for a random walk. Thus, in order to suppress the energy error ( $< 10^{-7}$ ) for  $\sim 10^6$  years, we should chose  $\Delta t/\tilde{R}_{\text{cut}} \lesssim 0.1$  (see also Fig. 4).



**Fig. 2.**  $N$ -body simulations of  $5 \times 10^3$  planetesimals for  $10^4$  yrs by using PENTACLE (solid) and a fourth-order Hermite scheme (dashed). Three colours correspond to three different random seeds for initial conditions of a planetesimal disc. Left: the number of remaining particles. Right: mass of the largest body.



**Fig. 3.** Cumulative distribution functions of the eccentricity (left panel) and inclination (right panel) of planetesimals at  $9 \times 10^3$  year.

More details about dependencies of accuracy on parameters are discussed in Oshino et al. (2011).

Figure 6 shows time evolution of relative energy errors to 100,000 Kepler times for model R with  $N = 10^6$ ,  $\theta = 0.5$ , and  $\eta = 0.1$ . We chose three different parameter sets of  $\tilde{R}_{\text{cut}}$  and  $\Delta t$ , such as  $\tilde{R}_{\text{cut}} = 0.3, \Delta t = 1/64$ ,  $\tilde{R}_{\text{cut}} = 0.5, \Delta t = 1/64$ , and  $\tilde{R}_{\text{cut}} = 0.3, \Delta t = 1/128$ . These results show that the increase in energy errors roughly obeys  $t^{1/2}$  over a long period of time.

### 3.2.2 Effect of disc radius

In order to investigate an effect of a disc radius on energy conservation, we also perform simulations similar to those in section 3.2.1 for model D with  $N = 10^6$ ,  $\theta = 0.5$ , and  $\tilde{R}_{\text{cut}} = 0.2, 0.3$ , and  $0.5$ . We adopt  $\Delta t = 1/64$  and  $1/128$  for these runs. The energy error is shown in Fig. 5, and the behaviour is similar to that of model R (see Fig. 7). This means that PENTACLE is applicable to  $N$ -body simulations for planet formation in a variety of disc models.

### 3.2.3 Efficiency for parallelization

We also discuss the performance and parallelization efficiency of PENTACLE. All the simulations in this section are carried out on Cray XC30 (ATERUI) at the Centre for Computational Astrophysics of the National Astronomical Observatory of Japan. ATERUI consists of 1,060 computer nodes and each node has two Intel Xeon E5-2690 v3 (12 cores, 2.6GHz) processors. We assigned one CPU core to one MPI process (i.e. the number of CPU cores  $N_c$  means that of MPI processes).

Fig. 8 shows the execution time per Kepler time for various  $N$  ( $8 \times 10^6, 10^6$ , and  $1.25 \times 10^5$ ). Each curve indicates different parameter sets of  $\Delta t$  and  $\tilde{R}_{\text{cut}}$ . For all the runs, we take  $\Delta t/\tilde{R}_{\text{cut}}$  to be constant so that the energy errors of different runs are almost the same. We see similar trends among most runs: the execution time decreases linearly for small  $N_c$  and increases for large  $N_c$ . To see more details, we plot the breakdown of the execution time for the run with  $N = 10^6$  (1M),  $\tilde{R}_{\text{cut}} = 0.6$ , and  $\Delta t = 1/32$  in Fig. 9. We see that the execution time for both the hard and soft parts decrease for small

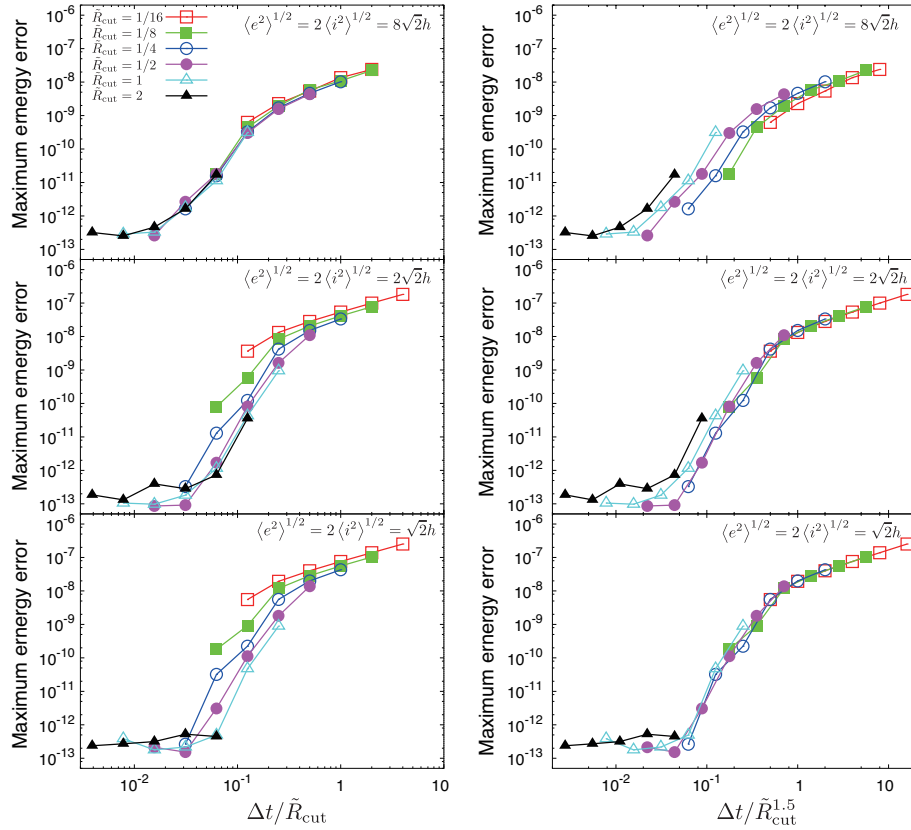


Fig. 4. Maximum energy error over ten Keplerian orbits as functions of  $\Delta t/\tilde{R}_{\text{cut}}$  (left panel) and  $\Delta t/(\tilde{R}_{\text{cut}})^{1.5}$  (right panel). Top, middle and bottom panels show results of hot, standard, and cold disc models, respectively.

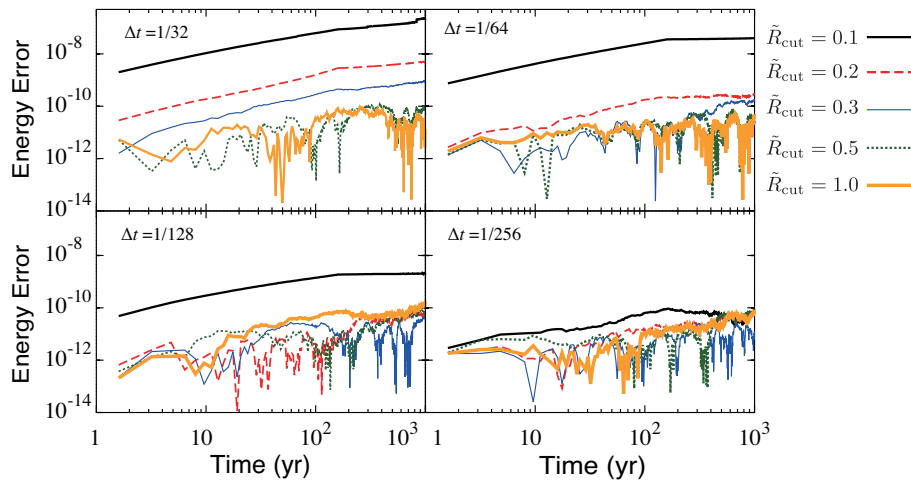


Fig. 5. Relative energy error as a function of time for model R with  $N = 10^6$  and  $\theta = 0.5$ :  $\tilde{R}_{\text{cut}} = 0.1$  (solid, black), 0.2 (dashed, red), 0.3 (thin solid, blue), 0.5 (dotted, green), and 1.0 (thick solid, orange). From the left top to the right bottom, we use  $\Delta t = 1/32, 1/64, 1/128,$  and  $1/256$ .

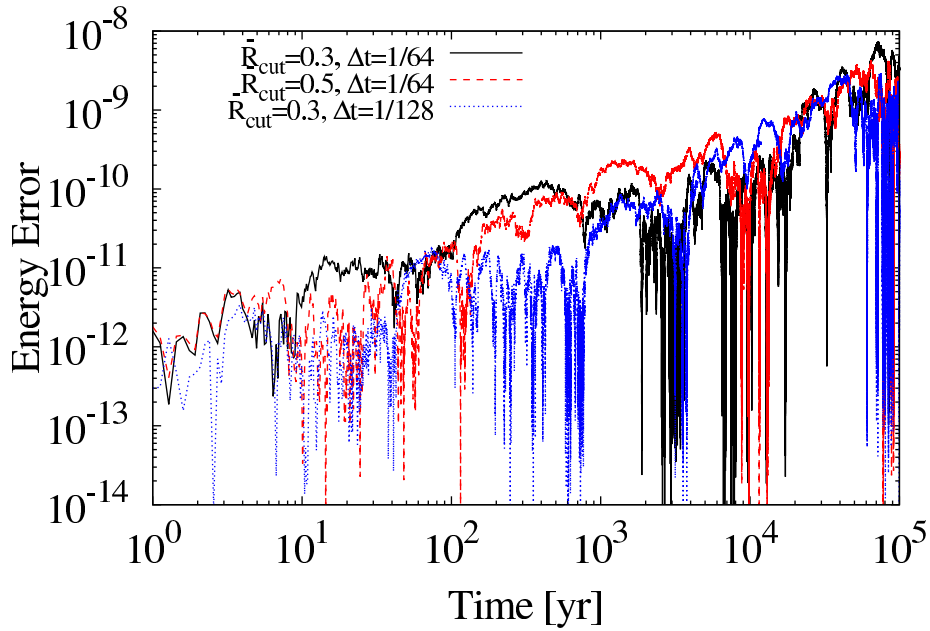


Fig. 6. Relative energy errors as a function of time for model R with  $N = 10^6$  and  $\theta = 0.5$ :  $\tilde{R}_{\text{cut}} = 0.3, \Delta t = 1/64$  (solid, black),  $\tilde{R}_{\text{cut}} = 0.5, \Delta t = 1/64$  (dashed, red), and  $\tilde{R}_{\text{cut}} = 0.3, \Delta t = 1/128$  (dotted, blue).

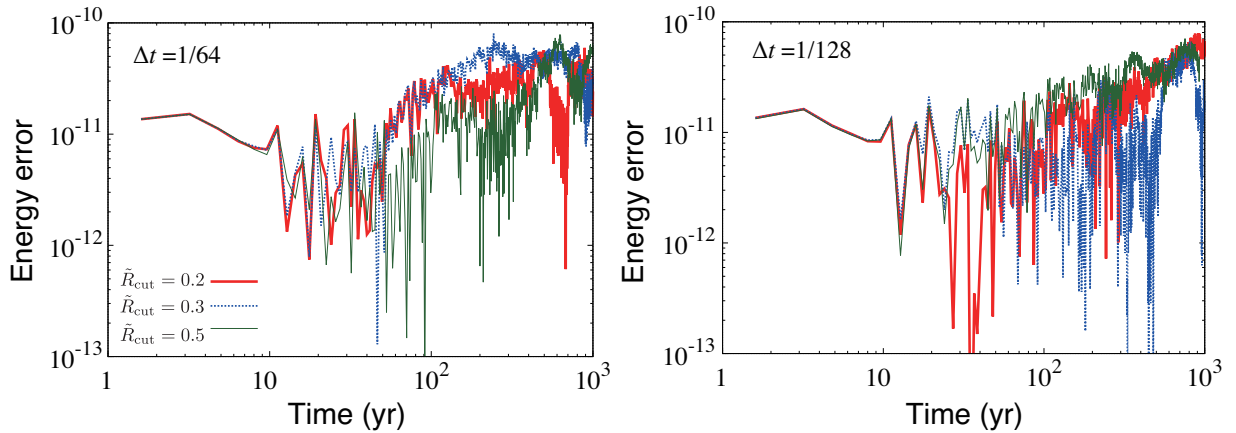


Fig. 7. Energy errors for model D with  $N = 10^6$  for  $\Delta t = 1/64$  (left) and  $1/128$  (right):  $\tilde{R}_{\text{cut}} = 0.2$  (thick solid, red),  $0.3$  (dotted, blue), and  $0.5$  (thin, green).

$N_c$ . However, as  $N_c$  increase, slopes for both parts become shallower and finally, the execution time for the hard (soft) part stalls (increases). For the hard part, we find a good scaling of the execution time for integrating particles in 1- and 2-clusters, whereas that for integrating particles in  $k_{>2}$ -clusters is independent of  $N_c$ . This is because the integration of  $k_{>2}$ -clusters is not executed in parallel. The time for gathering and scattering particles in  $k_{>2}$ -clusters from/to the root process is almost constant, because `MPI_Gatherv` and `MPI_Scatterv` used for gathering and scattering of particles are limited to the injection bandwidth. Thus, the minimum time for the hard part is limited to integrating or gathering (and scattering) particles in  $k_{>2}$ -cluster. For the soft part, the execution time for calculating a gravity force decreases linearly for all the range of  $N_c$ . However, the time for the exchange LET increases for large  $N_c$ . This is because

`MPI_Alltoallv` is used in FDPS at this step (Iwasawa et al. 2016).

We also show the same figure as Fig. 9, but with  $\tilde{R}_{\text{cut}} = 1.2$  and  $\Delta t = 1/16$ . behaviours of all the curves are similar those shown in Fig. 10, except that the hard part dominates the total execution time. Compared with the run with  $\tilde{R}_{\text{cut}} = 0.6$  and  $\Delta t = 1/32$ , more particles belong to  $k_{>2}$ -clusters in this case, in other words, many particles are not integrated in parallel. Figure 11 shows that the fraction of particles in 1-, 2-, and  $k_{>2}$ -clusters, and it indicates that the number of particle in  $k_{>2}$ -cluster is about one hundred times larger than that in 1-cluster. If, in the hard part, each execution time of integration of a particle per unit time is the same among all particles, the total execution time for the hard part can not be scaled for  $N_c \gtrsim 100$ . This conclusion is firmly supported by Fig. 10.



The execution time for the soft part of the run with  $\tilde{R}_{\text{cut}} = 1.2$  and  $\Delta t = 1/16$  is roughly half of that with  $\tilde{R}_{\text{cut}} = 0.6$  and  $\Delta t = 1/32$ . If we fully parallelize the hard part, its execution time is much smaller than the soft one. As a result, the total execution time of the run with  $\tilde{R}_{\text{cut}} = 1.2$  and  $\Delta t = 1/16$  roughly becomes half of that with  $\tilde{R}_{\text{cut}} = 0.6$  and  $\Delta t = 1/32$ .

Finally, we discuss a possibility of full parallelization of the hard part to permit a larger  $\tilde{R}_{\text{cut}}$  and  $\Delta t$ , namely, we reduce the number of the use of group communication per unit time. To discuss the possibility of full parallelization in the hard part, we plot the number of particles in the largest cluster against the mean number of neighbours per particle,  $\langle n_{\text{ngb}} \rangle$  in Fig. 13 and the distribution function of a cluster size, i.e.,  $k$ -cluster, in Fig. 14. As seen in Fig. 13, there is a threshold at  $\langle n_{\text{ngb}} \rangle \sim 1$ .

Under the circumstance of  $\langle n_{\text{ngb}} \rangle \lesssim 1$ , many clusters contain a few particles (see also Fig. 14). This means that we could integrate the particles in  $k_{>2}$ -cluster in parallel if we chose small enough  $\tilde{R}_{\text{cut}}$  to guarantee  $\langle n_{\text{ngb}} \rangle < 1$ . In addition, if we could integrate all the particles for the hard part in parallel, gathering (scattering) particles in  $k_{>2}$ -cluster to (from) the root process were not necessary<sup>2</sup>. Figure 14 also shows that the distribution function of a  $k$ -cluster depends on  $\langle n_{\text{ngb}} \rangle$  and is independent of  $N$ . The larger  $N$  we use, the more important the parallelization of the hard part becomes. Thus, we will modify PENTACLE to handle the hard part in fully parallel in the near future.

## 4 Terrestrial planet formation

In the previous section, we demonstrated that a high-resolution  $N$ -body simulation with one million particles for planet formation is doable if we use PENTACLE code. How does the growth of a planetary embryo proceed in a sea of "small" planetesimals? In order to investigate effects of the initial size of a planetesimal  $r_{\text{pls}}$ , we carried out three  $N$ -body simulations of terrestrial planet formation using  $N = 10^4$ ,  $10^5$ , and  $10^6$ , which correspond to  $r_{\text{pls}} \sim 507$  km, 235 km, and 109 km, respectively. We considered the same narrow planetesimal ring model as that used in Section 3.1. In these simulations, we introduce an aerodynamic drag force as described in Adachi et al. 1976. We assumed that an initial gas density at 1 au,  $\rho_0 = 2.0 \times 10^{-9}$  g cm<sup>-3</sup>. The density of a disc gas decreases exponentially with time in a manner of  $\rho_{\text{gas}} = \rho_0 \exp^{-t/1 \text{ Myrs}}$ , where  $\rho_{\text{gas}}$ ,  $t$  is the density of a disc gas and the time, respectively. We simulated planetesimal accretion onto a growing planetary embryo for 1 Myrs.

Figure 12 shows mass evolution of a largest body for 1 Myrs. We can see that a planetary embryo grows rapidly in a runaway fashion and its growth rate follows a power-law function of mass, as shown in Ida & Makino (1993). Then, the emergent runaway body enters the so-called oligarchic growth mode and

eventually, the final mass of the embryo approaches the almost same value in the three cases. We confirmed that a classical picture of terrestrial planet formation holds true for a swarm of equal-sized planetesimals with radius of  $\sim 100$  km. A significant difference among the three cases is, however, the duration of a transient phase between the runaway growth and the oligarchic growth. In the transient phase, the growth of a runaway body slows down but random velocities of ambient planetesimals are not excited so efficiently by itself yet. This may indicate that a planetary growth in a sea of smaller planetesimals proceeds in a non-equilibrium oligarchic growth mode, as suggested by Ormel et al. (2010) and Kobayashi et al. (2010). This topic will be discussed in our forthcoming paper. Last but not the least, although energy errors of the high-resolution  $N$ -body simulation are not shown in this paper, they are always lower than  $10^{-7}$ .

## 5 Discussions and Summary

We have developed a parallelized hybrid  $N$ -body code (PENTACLE) to perform high-resolution simulations of planet formation. The open-source library designed for full automatic parallelization of particle simulations (FDPS) is implemented in PENTACLE. PENTACLE uses a 4th-order Hermite scheme to calculate gravitational interactions from particles within a cut-off radius ( $\tilde{R}_{\text{cut}}$ ) and the Barnes-Hut tree method for gravity from particles beyond. We also confirmed that results of planetary growth in a planetesimal ring using PENTACLE are in good agreement with those using a direct  $N$ -body code.

We figured out that  $\Delta t/\tilde{R}_{\text{cut}} \lesssim 0.1$  reduces energy errors to an acceptable level when simulating planetary accretion in a swarm of planetesimals (see Figs. 4 – 7). PENTACLE allows us to handle 1 – 10 million particles in a collisional system; for example, on a supercomputer with  $10^3$  CPU cores, it takes one month to trace the dynamical evolution of  $10^6$  planetesimals for 1 Myr. Nevertheless, as shown in Fig. 8, the computational cost of runs with  $10^7$  or more particles would be still expensive. The bottleneck of the performance for larger  $N_c$  (the number of CPU cores) is the exchange LET used for MPI\_Alltoallv. In order to relax this problem, we could reduce the number of processes due to the usage of accelerators such as GRAPE, GPU or PEZY-SC, while keeping the peak performance. We are now developing a GPU-enable version, PENTAGLE (a Parallelized Particle-Particle Particle-tree code for Planet formation on a GPU cluster) based on Iwasawa et al. (2015).

We have focused the scope of this paper on the performance and accuracy of PENTACLE, but have also demonstrated the mass evolution of a planetary embryo embedded in a disc with  $10^6$  planetesimals. Increasing the number of particles used in an  $N$ -body simulation decreases their sizes, namely the physical size of a planetesimal. A random velocity distribution of plan-

<sup>2</sup> Inter-adjacent node communications are still required but these costs would be much smaller than the collective one

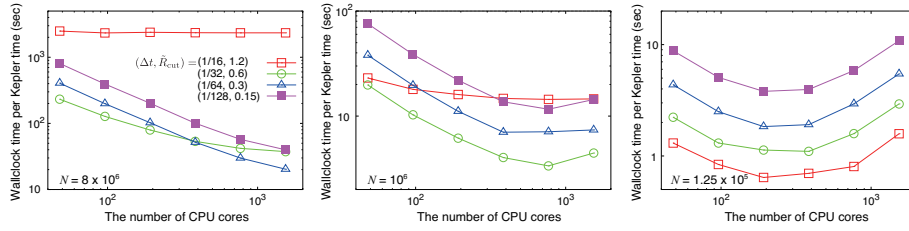


**Fig. 8.** Execution time per Kepler time for  $N = 8 \times 10^6$  (left panel),  $10^6$  (middle panel), and  $1.25 \times 10^5$  (right panel) against the number of CPU cores. Symbols correspond to different  $\Delta t$  and  $\tilde{R}_{\text{cut}}$ .

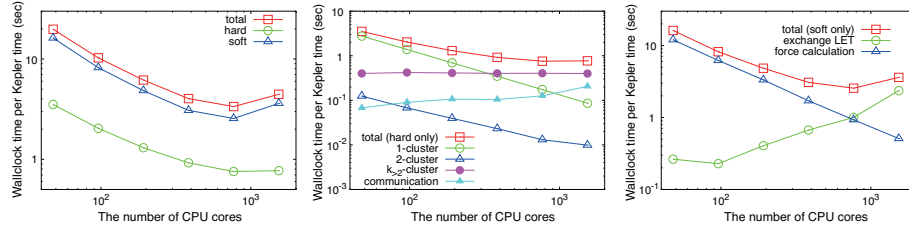


**Fig. 9.** Breakdown of the execution time for the runs with  $N = 1M$ ,  $\tilde{R}_{\text{cut}} = 0.6$  and  $\Delta t = 1/32$ . Left panel: breakdown of the total execution time against the number of CPU cores. Open squares, open circles, and open triangles indicate the total execution time, the hard-part one, and the soft-part one, respectively. Middle panel: breakdown of the execution time for the hard-part. Open squares indicate the total execution time for the hard part only. Open circles, open triangles and filled circles indicate the time for integrating particles in 1-, 2- and  $k_{>2}$ -cluster, respectively. Filled triangles indicate the time for both gathering and scattering particles in  $k_{>2}$ -cluster from/to the root processes. Right panel: breakdown of the execution time for the soft-part. Open squares indicate the total execution time for the soft part only and open circles and open triangles indicate the time for the exchange LET and the force calculation using the tree method, respectively.

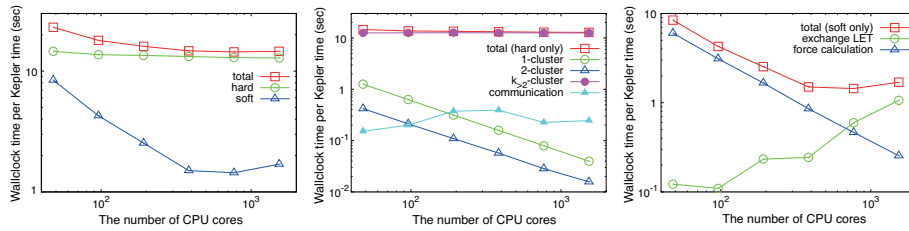


**Fig. 10.** The same figures as Fig. 9, but with  $\tilde{R}_{\text{cut}} = 1.2$  and  $\Delta t = 1/16$ .

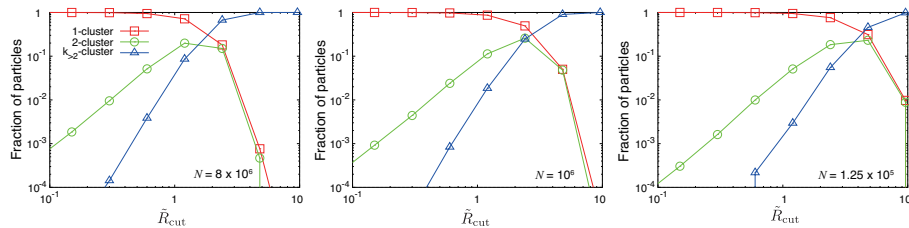


**Fig. 11.** Fraction of particles in 1- (red open square), 2- (green open circle) and  $k$ -clusters (blue open triangle) against  $\tilde{R}_{\text{cut}}$  for the runs with  $N = 8 \times 10^6$  (left panel),  $10^6$  (middle panel), and  $1.25 \times 10^5$  (right panel).

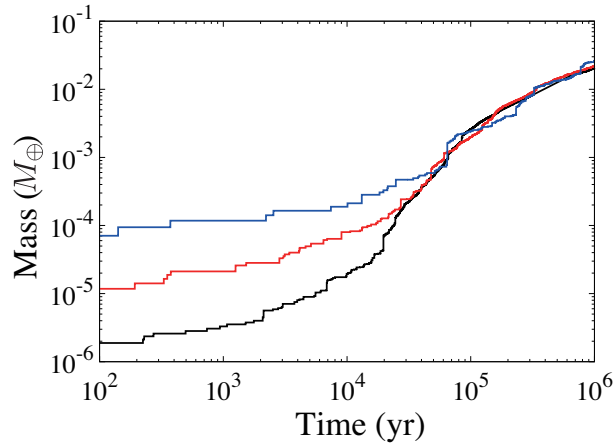


**Fig. 12.** Mass evolution of the largest planetary embryo in  $N$ -body simulations with  $N = 10^4$  (blue),  $10^5$  (red), and  $10^6$  (black) planetesimals, which correspond to  $r_{\text{pls}} \sim 507$  km, 235 km, and 109 km, respectively.

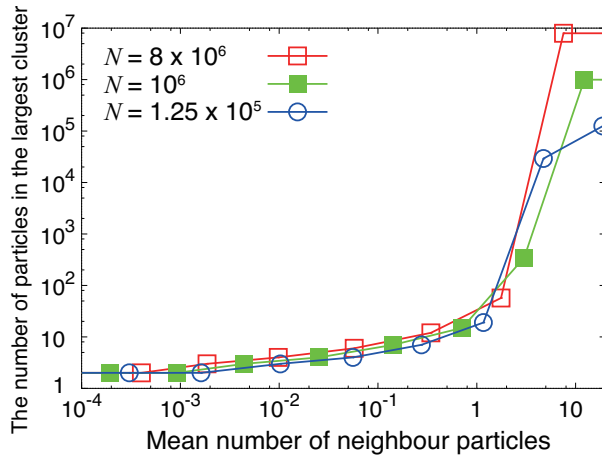


**Fig. 13.** The number of particles in the largest cluster against the mean number of neighbours per particle for the runs with  $N = 8 \times 10^6$  (red open square),  $10^6$  (green filled square), and  $1.25 \times 10^5$  (blue open circle).

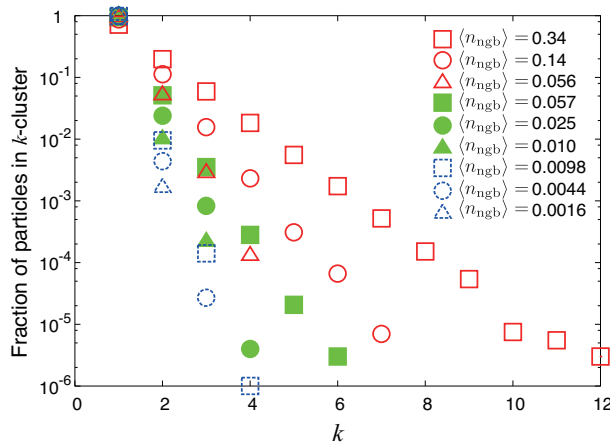


**Fig. 14.** Fraction of particles in a  $k$ -cluster for runs with  $\tilde{R}_{\text{cut}} = 1.2$  (red, open), 0.6 (green, full), and 0.3 (blue, dashed) for  $N = 8 \times 10^6$  (square),  $10^6$  (circle), and  $1.25 \times 10^5$  (triangle).

etesimals in both a runaway and oligarchic growth mode could become different. This means that the growth of a planetary embryo in a sea of small planetesimals might proceed unlike a traditional picture of terrestrial planet formation. This topic will be discussed in our next paper.

PENTACLE will be freely available under the MIT license for all those who interested in large-scale particle simulations. The source code is hosted on the GitHub platform and can be downloaded from <https://github.com/PENTACLE-Team/PENTACLE>. The next version will be executable on a GPU cluster and also we will include effects of disc-planet interactions and a statistical treatment of collisional fragmentation into PENTACLE.

## Acknowledgments

This project was supported by JSPS KAKENHI Grant Numbers 15H03719. Y.H. and M.F. were supported by JSPS KAKENHI Grant Numbers 26800108 and 26103711, respectively.  $N$ -body simulations in this paper were carried out on Cray XC30 (ATERUI) at the Centre for Computational Astrophysics of the National Astronomical Observatory of Japan. This research used computational resources of the K computer provided by the RIKEN Advanced Institute for Computational Science through the HPCI System Research project (Project ID:ra000008). Part of the research covered in this paper research was funded by MEXT's program for the Development and Improvement for the Next Generation Ultra High-Speed Computer System, under its Subsidies for Operating the Specific Advanced Large Research Facilities.

## References

- Aarseth, S. J. 1963, *MNRAS*, 126, 223
- Adachi, I., Hayashi, C., & Nakazawa, K. 1976, *Progress of Theoretical Physics*, 56, 1756
- Bagla, J. S. 2002, *Journal of Astrophysics and Astronomy*, 23, 185
- Barnes, J., & Hut, P. 1986, *Nature*, 324, 446
- Bédorf, J., Gaburov, E., & Portegies Zwart, S. 2015, *Computational Astrophysics and Cosmology*, 2, 8
- Bottke, W. F., Durda, D. D., Nesvorný, D., et al. 2005, *Icarus*, 175, 111
- Bromley, B. C., & Kenyon, S. J. 2006, *AJ*, 131, 2737
- Chambers, J. E. 1999, *MNRAS*, 304, 793
- Chambers, J. 2008, *Icarus*, 198, 256
- Dubinski, J., Kim, J., Park, C., & Humble, R. 2004, *New Astronomy*, 9, 111
- Duncan, M. J., Levison, H. F., & Lee, M. H. 1998, *AJ*, 116, 2067
- Grimm, S. L., & Stadel, J. G. 2014, *ApJ*, 796, 23
- Hayashi, C. 1981, *Progress of Theoretical Physics Supplement*, 70, 35
- Hockney, R. W., & Eastwood, J. W. 1981, *Computer Simulation Using Particles*, New York: McGraw-Hill, 1981,
- Ida, S., & Makino, J. 1992, *Icarus*, 96, 107
- Ida, S., & Makino, J. 1993, *Icarus*, 106, 210
- Inaba, S., Tanaka, H., Nakazawa, K., Wetherill, G. W., & Kokubo, E. 2001, *Icarus*, 149, 235
- Ishiyama, T., Fukushige, T., & Makino, J. 2009, *PASJ*, 61, 1319
- Iwasawa, M., Portegies Zwart, S., & Makino, J. 2015, *Computational Astrophysics and Cosmology*, 2, 6
- Iwasawa, M., Tanikawa, A., Hosono, N., et al. 2016, *PASJ*, 68, 54
- Kinoshita, H., Yoshida, H., & Nakai, H. 1991, *Celestial Mechanics and Dynamical Astronomy*, 50, 59
- Kobayashi, H., Tanaka, H., Krivov, A. V., & Inaba, S. 2010, *Icarus*, 209, 836
- Kobayashi, H., Tanaka, H., & Krivov, A. V. 2011, *ApJ*, 738, 35
- Kokubo, E., & Ida, S. 1998, *Icarus*, 131, 171
- Levison, H. F., Duncan, M. J., & Thommes, E. 2012, *AJ*, 144, 119
- Makino, J. 1991, *ApJ*, 369, 200
- Makino, J., & Aarseth, S. J. 1992, *PASJ*, 44, 141
- Makino, J., Kokubo, E., & Taiji, M. 1993, *PASJ*, 45, 349
- Makino, J., Fukushige, T., Koga, M., & Namura, K. 2003, *PASJ*, 55, 1163
- Morishima, R. 2015, *Icarus*, 260, 368
- Ormel, C. W., Dullemond, C. P., & Spaans, M. 2010, *ApJL*, 714, L103
- Oshino, S., Funato, Y., & Makino, J. 2011, *PASJ*, 63, 881
- Richardson, D. C., Quinn, T., Stadel, J., & Lake, G. 2000, *Icarus*, 143, 45
- Springel, V. 2005, *MNRAS*, 364, 1105
- Stadel, J. G. 2001, Ph.D. Thesis, 3657
- Sugimoto, D., Chikada, Y., Makino, J., et al. 1990, *Nature*, 345, 33
- Wang, L., Spurzem, R., Aarseth, S., et al. 2015, *MNRAS*, 450, 4070
- Weidenschilling, S. J., Spaute, D., Davis, D. R., Marzari, F., & Ohtsuki, K. 1997, *Icarus*, 128, 429
- Wetherill, G. W., & Stewart, G. R. 1989, *Icarus*, 77, 330
- Wisdom, J., & Holman, M. 1991, *AJ*, 102, 1528
- Xu, G. 1995, *ApJS*, 98, 355
- Yoshikawa, K., & Fukushige, T. 2005, *PASJ*, 57, 849